Global Change Biology (2005) **11,** 1101–1117, doi: 10.1111/j.1365-2486.2005.00975.x

# Land-use change and water losses: the case of grassland afforestation across a soil textural gradient in central Argentina

MARCELO D. NOSETTO*†, ESTEBAN G. JOBBÁGY* and JOSÉ M. PARUELO‡

*Grupo de Estudios Ambientales – IMASL, Universidad Nacional de San Luis & CONICET, Avenida Ejercito de los Andes 950 (D5700HHW), San Luis, Argentina, †Facultad de Ciencias Agropecuarias, Universidad Nacional de Entre Ríos. Ruta 11 km 10 Oro Verde (E3100XAD) Entre Ríos, Argentina, ‡IFEVA – Facultad de Agronomía, Universidad de Buenos Aires & CONICET, Avenida San Martín 4453, (C1417DSE) Ciudad de Buenos Aires, Argentina

**Abstract**

**Vegetation changes, particularly those involving transitions between tree- and grass-dominated covers, often modify evaporative water losses as a result of plant-mediated shifts in moisture access and demand. Massive afforestation of native grasslands, particularly important in the Southern Hemisphere, may have strong yet poorly quantified effects on the hydrological cycle. We explored water use patterns in *Eucalyptus grandis* plantations and the native humid grasslands that they replace in Central Argentina. In order to uncover the interactive effects that land cover type, soil texture and climate variability may have on evaporative water losses and water use efficiency, we estimated daily evapotranspiration (ET) in 117 tree plantations and grasslands plots across a soil textural gradient (clay-textured Vertisols to sandy-textured Entisols) using radiometric information from seven Landsat scenes, existing timber productions records, and $^{13}C$ measurements in tree stems. Tree plantations had cooler surface temperatures ($-5\,^{\circ}C$ on average) and evaporated more water ($+80\%$ on average) than grasslands at all times and across all sites. Absolute ET differences between grasslands and plantations ranged from $\sim 0.6$ to $2\,mm\,day^{-1}$ and annual up-scaling suggested values of $\sim 630$ and $\sim 1150\,mm\,yr^{-1}$ for each vegetation type, respectively. The temporal variability of ET was significantly lower in plantations compared with grasslands (coefficient of variation 36% vs. 49%). Daily ET increased as the water balance became more positive (accumulated balance for previous 18 days) with a saturation response in grassland vs. a continuous linear increase in plantations, suggesting lower ecophysiological limits to water loss in tree canopies compared with the native vegetation. Plantation ET was more strongly affected by soil texture than grassland ET and peaked in coarse textured sites followed by medium and fine textured sites. Timber productivity as well as $^{13}C$ concentration in stems peaked in medium textured sites, indicating lower water use efficiency on extreme textures and suggesting that water limitation was not responsible for productivity declines towards finer and coarser soils. Our study highlighted the key role that vegetation type plays on evapotranspiration and, therefore, in the hydrological cycle. Considering that tree plantations may continue their expansion over grasslands, problematic changes in water management and, perhaps, in local climate can develop from the higher evaporative water losses of tree plantations.**

*Keywords:* ecohydrology, eucalyptus, evapotranspiration, Landsat, remote sensing, vegetation change, water use efficiency, water yield

*Received 7 September 2004; revised version received 18 March 2005 and accepted 21 March 2005*

Correspondence: M. D. Nosetto, Grupo de Estudios Ambientales. IMASL–Universidad Nacional de San Luis, Avenida Ejercito de los Andes 950,(D5700HHW) San Luis, Argentina. tel. (+54) 2652 422803 int 229, e-mail: mnosetto@unsl.edu.ar

 

## Introduction

As a major component of the Earth's energy balance, evapotranspiration (ET) influences the behavior of the planetary boundary layer, mesoscale circulation patterns, and weather (Kelliher *et al.*, 1993). ET is also a large component of the Earth's hydrologic cycle explaining 60% of continental precipitation (Brutsaert, 1986). Plants, through their capacity to access, transport, and evaporate water, exert a strong control on the ET process (Calder, 1998), and vegetation changes, particularly those involving transitions between tree- and grass-dominated covers, often alter ET (Horton, 1919; Bosch & Hewlett, 1982; Zhang *et al.*, 2001). Transpiration, which is the principal component of ET over most of the land surface, is strongly coupled with the rate of carbon assimilation, and thus with primary productivity (Monteith, 1988). In this paper, we explore the ET patterns of eucalyptus plantations and the native humid grasslands that they are replacing in a heavily afforested area of Central Argentina.

ET varies with vegetation as a result of plant effects on water demand and supply. Under wet conditions, ET is principally limited by the atmospheric demand of water vapor, driven by advection and radiation, whereas under dry conditions ET is mainly limited by soil water supply, with the importance of these controls changing with the type of vegetation (Calder, 1998). The high aerodynamic roughness of forests allows the exchange of heat and water vapor between the canopy surface and the air to occur at rates up to 10 times higher than those possible for shorter vegetation, creating contrasting ET patterns under wet conditions (Kelliher *et al.*, 1993; Calder, 1998). Under a sufficient water supply, the higher capture of advective energy in forest canopies translates into higher evaporative water losses than those achieved by shorter herbaceous canopies, which maintain ET more closely coupled to the supply of radiant energy. Under drier conditions, the availability of soil moisture becomes the primary control of ET, and differences in the capacity of plants to access water, often dictated by rooting depth, can result in contrasting evaporative losses across vegetations types (Calder, 1998). Trees tend to have deeper roots than herbaceous plants (Canadell *et al.*, 1996; Schenk & Jackson, 2002), and hence can maintain higher ET than grasslands when the water supply declines (Calder *et al.*, 1997; Sapanov, 2000).

Contrasting evaporative water losses between tree plantations and grasslands have been evidenced by a diverse array of approaches such as plot studies showing drier soil and vadose zones under the former (Calder *et al.*, 1993, 1997), paired watershed experiments showing decreased streamflow when grassland watersheds are afforested (Sahin & Hall, 1996; Scott & Lesch, 1997), and groundwater observations revealing the onset of phreatic water discharge under afforested plots within herbaceous landscapes (Heuperman, 1999; Sapanov 2000; Jobbagy & Jackson 2004).

As a key determinant of water storage and transport, soil texture has a strong influence on ET, interacting with vegetation type in multiple ways (Noy-Meier, 1973; Hillel, 1998). Under humid and subhumid conditions, medium textured soils present the highest available water for plants because they pose an optimum compromise between the low water holding capacity and high drainage losses of coarse textured soils and the poor infiltration and high runoff of fine textured soils. Vegetation can affect this relationship if, for example, the greater rooting depth of trees compared with grasses (Schenk & Jackson, 2002) restricts deep drainage losses in coarse textured soils and allows ET rates comparable with those of medium textured soils. In addition, soil texture can affect ET in an indirect way through its influence on other resources and factors important for plants. For example, nutrient limitation associated with the low ion exchange capacity of coarse soils or oxygen limitations related to the poor aeration of fine soils can limit ET through their negative effect on plant growth.

In southern South America, large areas still covered by native grasslands are being converted to forests at very high rates. This conversion, namely grassland afforestation, is often motivated by governmental policies (Richardson, 1998; Geary, 2001) and will very likely be reinforced by the prospective carbon sequestration market in the future (IGBP TCWG, 1998; Wright *et al.*, 2000). As examples, in Uruguay, the rate of afforestation increased from $2500\,\mathrm{ha\,yr^{-1}}$ in the 1975–1988 period to $\sim 50\,000\,\mathrm{ha\,yr^{-1}}$ in the last decade (FAO, 2001). In Argentina, these rates jumped from $\sim 30\,000\,\mathrm{ha\,yr^{-1}}$ in 1996 to $\sim 100\,000\,\mathrm{ha\,yr^{-1}}$ in 2001 (SAGPyA, 2002). Eucalyptus and pines are the most common species in these plantations. In the mid-Uruguay river basin, the most heavily afforested grassland area of Argentina, *Eucalyptus grandis* plantations dominate a broad gradient of soil texture along which their productivity displays strong variation, peaking at medium textured soils and decreasing towards coarser and finer textured ones (Marcó, 1988a; Sepliarsky & Dalla Tea, 1993).

In this paper, we explore water use patterns in *E. grandis* plantations and native grasslands in the mid-Uruguay River basin of Argentina focusing on the interactions of vegetation type, soil texture, and climate variability on ET and water use efficiency. Acknowledging that afforested landscapes are a mosaic of plantations of different ages, we also characterize ET

changes with age across plots ranging from planting to harvesting stages.

The following hypotheses guided our work and provided predictions that we evaluate with our data:

(1) Tree plantations consume more water than native grasslands during dry and wet periods because of their greater capacity to access soil water and to exchange vapor with the atmosphere. ET is expected to be higher and more stable through time in tree plantations in comparison with native grasslands in the same environments.
(2) Tree plantations show lower declines of water consumption towards coarse textured soils compared with native grasslands because their greater rooting depth prevents part of the large drainage losses of these soils. On the contrary, water consumption declines similarly for grasslands and tree plantations towards fine textured soils because the poor infiltration and high runoff affect both covers as well. ET is expected to peak in medium textured soils for both types of vegetation and shows minimum values in clay soils for plantations and in sandy soils for grasslands.
(3) (A) The declines of tree production that are typically observed from medium textured soils towards fine and coarse textured soils (Marcó, 1988a; Sepliarsky & Dalla Tea, 1993) are caused by water limitation. As a result, we expected increased water use efficiency (biomass production per unit of transpired water) of tree plantations towards soils with extreme textures. (B) Alternatively, production declines in coarse and fine textured soils are explained by nonwater-related constrains. In this case we expect a decline in water use efficiency of tree plantations towards extreme textures.

To explore these hypotheses, we assessed ET rates in 117 tree plantation and native grassland plots over a $\sim 3500\,km^2$ area encompassing a broad, yet spatially compact, soil texture gradient (clay-textured Vertisols to sandy-textured Entisols) based on thermal information from seven Landsat scenes. We evaluated water use efficiency based on our remote estimates of ET and existing production records and we complemented them with measurements of stable isotopes of carbon in tree stems. As an independent measure of water consumption at the catchment scale, we analyzed existing stream chloride data and its relation with the proportion of watersheds that was afforested.

## Materials and methods

### *Study region*

We performed our study on the western coast of the mid-Uruguay river in Argentina, between latitudes 30°49′S and 31°43′S and longitudes 58°34′W and 57°55′W (Fig. 1). The region has a humid warm-

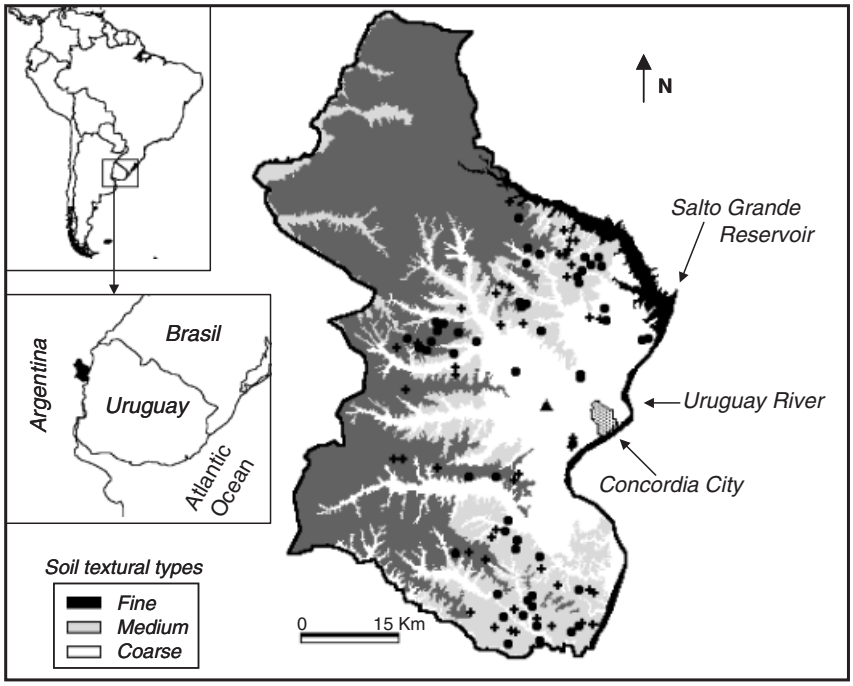


**Fig. 1** Study region. Distribution of tree plantation and grassland plots are indicated with spots and crosses, respectively. The location of the meteorological station is indicated with a triangle. Soil types were obtained from 1:100 000 maps by INTA (1993).

temperate climate with a mean annual temperature of 18.5 °C and mean temperatures for the coldest (July) and warmest (January) months of 12.3 °C and 25 °C, respectively. Mean precipitation in the city of Concordia is 1352 mm $yr^{-1}$ (1979–2003) with 60% of it occurring during spring and summer (October–March). Mean pan evaporation is 1538 mm $yr^{-1}$ with 72% occurring during spring and summer. The region has a rolling landscape ranging from 5 to 70 m of altitude above sea level. Soils developed on sedimentary materials of fluvial, aeolian, and lacustrine origin. On the eastern side of the study area, next to the Uruguay River, soils developed on quartziferous sand and gravel transported by the river, and have sandy texture with $\sim 70$ mm $m^{-1}$ of water-holding capacity. These soils are classified as Udifluvents and Quartzipsamments (Yuquerí Chico and Yuquerí Grande series). On the western side of the study area, soils developed on lacustrine sediments and have clay contents ranging between 30% and 45% with $\sim 160$ mm $m^{-1}$ of water-holding capacity. These soils are classified as Pelluderts (Yeruá, Yaros, and San Buenaventura series). Between the previous groups of soils there is a belt of medium textured soils developed on fluvial sediments deposited over lacustrine materials with sandy to sandy-loam topsoils and a clay horizon at 40–70 cm depth. These soils have $\sim 110$ mm $m^{-1}$ of water-holding capacity and are classified as Argiudols, Hapludols, and Haplumbreptes (Mandisoví, Los Charruas, Calabacilla, and Puerto Yeruá series). Groundwater in the area is located between 2 and 35 m below the ground surface (INTA, 1984, 1993).

Most of the region was originally dominated by grasses with a mixture of $C_3$ and $C_4$ species of the genera *Paspalum*, *Axonopus*, *Stipa*, *Bromus*, and *Piptochaetium* (Landi *et al*., 1987). Since the 1940s, when the first commercial tree plantations were established, afforestation became one of the dominant land uses of the area, with *E. grandis* Hill ex Maiden, *Pinus elliotti* Engelm., and *Pinus taeda* L. being the most widespread species in order of importance. Currently, this region is one of the most heavily afforested areas of southern South America, with 91 100 and 10 500 ha of eucalyptus and pine plantations, respectively (Brizuela *et al*., 2003). *E. grandis* plantations achieve the highest wood productions in the area, ranging between 25 and 55 $m^3$ $ha^{-1}$ $yr^{-1}$ and peaking in medium textured soils (Marcó 1988a; Sepliarsky & Dalla Tea 1993).

Eucalyptus is usually cultivated with densities of 1000–1100 trees $ha^{-1}$ ($3 \times 3$ or $4 \times 2.5$ $m^2$ spacing) and subject to coppice management. Plantations are clearcut 10–12 years after planting and let to regrow for two consecutive shifts of similar duration. Weeds are usually controlled either mechanically or chemically in the first 2 years. The great majority of wood production from these plantations is used for trituration (cellulose and boards, 60%) and sawmills (38%) (INTA, 1995; SAGPyA, 1999).

### *Study sites and satellite images*

To evaluate ET and radiation interception patterns of grasslands and tree plantations, we selected plots of more than 10 ha occupied by first generations of *E. grandis* plantations of 8–11 years of age (52 plots) and native grassland (48 plots) distributed across the soils texture gradient and grouped as coarse, medium, and fine textured, according to the soil map of the region (1 : 100 000) (INTA, 1993) (Fig. 1). We included a set of 17 coastal, coarse textured sites with *E. grandis* plantation and native grasslands plots located $<1000$ m away from the shores of the Salto Grande reservoir and Uruguay River to explore potential groundwater use by trees in this zone, where the water table is shallowest ($<10$ m below the ground) and groundwater transport warranted by the high hydraulic conductivity of sediments (Jobbagy & Jackson, 2004). To characterize ET and radiation interception changes with tree plantations age, we selected an independent set of 31 *E. grandis* plots located in medium textured soils that ranged from land preparation/planting to harvesting stages. The age of plantations was obtained from a sequence of 16 Landsat and SAC-C images covering the study region from 1985 to present. To avoid edge effects on the data from satellite images, we used core pixels of each plot excluding a $\sim 60$ m wide edge zone.

We used seven cloud-free Landsat 7 ETM + images provided by CONAE (path 225, row 82) covering our entire study region. Scenes were acquired at 10 : 30 hours (local time) on 08/30/00, 11/18/00, 02/06/01, 04/11/01, 07/19/02, 12/26/02, and 01/27/03. These cloud-free dates covered a broad range of water availability conditions, as suggested by rainfall–open pan evaporation water balances (Fig. 2c). Images were geometrically corrected using the control point selection method with a second-order polynomial warp function (mean square error for the transformation $<1$ pixel) (Eastman, 1999). In order to minimize atmospheric effects, nonthermal bands were corrected using a dark object subtraction (DOS) approach described by Chavez (1989), and the thermal band was corrected using the mono-window algorithm proposed by Qin *et al*. (2001).

### *ET estimates*

We assessed actual daily ET rates and radiation interception by canopies based on Landsat 7 images

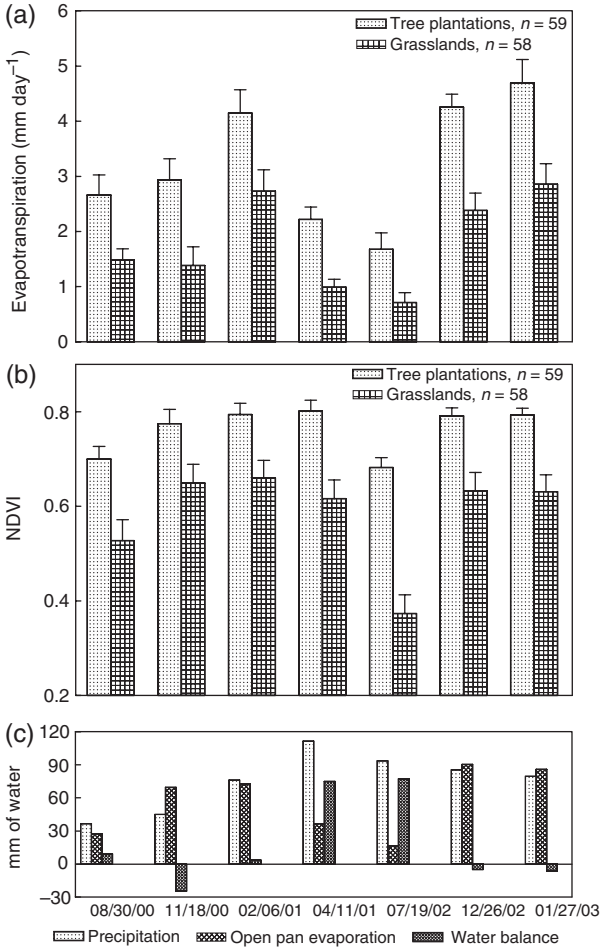


**Fig. 2** Evaporative water losses and radiation interception in *Eucalyptus grandis* plantations and native grasslands across seven dates. Actual evapotranspiration (ET) (a) and NDVI (b) were computed from Landsat images. Differences between both covers were always significant ($P<0.01$). Bars correspond to standard deviation. Precipitation (P), open pan evaporation (OPE) and water balance (WB = P–OPE) integrated for the 18 previous days to the image acquisition date are shown (c).

with a spatial resolution of 30 m for nonthermal bands and 60 m for the thermal band. We estimated daily ET using surface radiant temperature measurements based on the so-called Simplified Method (Jackson *et al*., 1977, see also Carlson & Buffum, 1989; Caselles *et al*., 1998). This method calculates daily ET considering the net radiation received by the surface and its temperature difference with the surrounding air mass based on the following equation (Jackson *et al*., 1977; Carlson *et al*., 1995):

$$\mathrm{ET}_{24} = \mathrm{Rn}_{24} - B(T_s - T_a)^n,$$

where $\mathrm{ET}_{24}$ (mm day$^{-1}$) and $\mathrm{Rn}_{24}$ (mm day$^{-1}$) are, respectively, the integrated actual ET and net radiation over a 24 h period, $T_s$ (K) the surface radiant temperature, $T_a$ (K) the 50 m air temperature above ground level, and $B$ (mm day$^{-1}$ K$^{-1}$) and $n$ parameters that vary with vegetation type. Although this method is simple, it also has a strong physical basis and has been successfully applied for different vegetation types (crops, grasslands, forests) (Seguin & Itier 1983; Brasa Ramos *et al*., 1996; Caselles *et al*., 1998; Sanchez & Caselles 2004).

Net radiation (Rn) values were obtained semi-empirically calculating the total incoming short-wave radiation (St) based on the approach described by Shuttleworth (1993) and computing surface albedo ($\alpha$) from bands 1 (blue), 3 (red), 4 (near-infrared), 5, and 7 (middle-infrared) of Landsat images following the method proposed by Liang (2000). These two values were used to estimate net short-wave radiation (Sn) (Appendix A). The net long-wave radiation (Ln) was estimated empirically from St according to Granger & Gray (1990) and summed to Sn to provide Rn. Temperature difference ($T_s - T_a$) estimates were based on surface temperature ($T_s$) calculation derived from band 6 of Landsat images according to the algorithm proposed by Qin *et al*. (2001) and 50 m air temperature ($T_a$), which was estimated from 1.5 m air temperature registered in a meteorological station located in the center of the study region according to Campbell & Norman (1998). Coefficients $B$ and $n$ were obtained from a scaled vegetation index (NDVI*) computed from bands 3 and 4 of Landsat images according to the procedure described by Carlson *et al*. (1995) (Appendix A).

### *Sensitivity analysis and validation*

The sensitivity analysis of the ET model focused on the variation of ET differences between tree plantations and grassland to changes in the $B$ parameter and surface temperature ($T_s$). This evaluation was performed on two dates (11/18/2000 dry and 02/06/2001 humid). Acknowledging that the $B$ parameter is crucial in the model and that it is currently more uncertain for forests (Sanchez & Caselles, 2004) than for grasslands (Seguin *et al*., 1982; Seguin & Itier, 1983; Vidal *et al*., 1987; Lagouarde & Brunet, 1989; Hurtado *et al*., 1994), we explored the effect of extreme $B_{\mathrm{forest}}$ values ($B_{\mathrm{forest}} = B_{\mathrm{grassland}}$ in the low end and a raise of 25% in the high end). To account for possible errors on $T_s$ estimation, we tested ET sensitivity to this variable by varying it $\pm 1$ K in both types of vegetation.

In order to compare our remote estimates of ET with more detailed ET data, sap flux measurements were carried out from 12 to 22 December 2003 in an *E. grandis* plot located within the study region. The plot, located on coarse textured soil, represented typical plantations

of the study region. Trees were planted in 1996 (8 years of age at the time of our measurements) with a density of 1111 plants $ha^{-1}$ ($3 \times 3$ spacing). Hole digging for individual plants was the only disturbance associated with tree establishment. Heat dissipation sapflow sensors (Granier, 1987) were installed in 10 trees distributed among the different size classes. Temperature differentials between the heated and reference probes were measured every 10 s and integrated for 30 min periods with a datalogger (CR10X; Campbell Scientific Inc., North Logan, UT, USA). Values were transformed to sap flux density ($U$, kg $H_2O$ $m^{-2}$ sapwood area $s^{-1}$) according to Granier (1985). Canopy transpiration was calculated as the product between $U$ and sap wood area.

*Photosynthetic radiation interception*

Red and near-infrared spectral information is strongly related with the fraction of the incoming photosynthetically active radiation intercepted (FPAR) by green vegetation (Sellers, 1985; Choudhury, 1987). We estimated FPAR in grasslands and tree plantations from NDVI using the formula presented by Ruimy *et al.* (1994):

$$\mathrm{FPAR} = 0.025 + 1.25\mathrm{NDVI}.$$

*Climate and productivity data*

Daily rainfall, open pan evaporation, wind speed, relative humidity and bright sunshine hours per day as well as hourly temperatures were obtained from a meteorological station located in the vicinity of Concordia, within the study area (−31°22′; −58°07′). We used these data to calculate rainfall–open pan evaporation water balances before and at each date of image acquisition. In order to evaluate differences in wood productivity among soil textural types, we compiled existing data from five local studies based on *E. grandis* plantations 7–14 years of age (Marcó, 1988a, b; Sepliarsky & Dalla Tea, 1993; Goya *et al.*, 1997; Frangi *et al.*, 2000).

*$^{13}C$ analysis*

We evaluated water use efficiency as an indicator of water limitation across the soil textural gradient by measuring the concentration of $^{13}C$ in tree stems at 14 stands of *E. grandis*. The concentration of $^{13}C$ in plant tissues is strongly affected by the intercellular concentration of $CO_2$ and has been successfully related with water use efficiency (Farquhar *et al.*, 1982). Stomatal closure, often associated with water deficits, results in an improvement of the intrinsic water use efficiency and a reduction of $[CO_2]$ in the stomatal cavity that leads to lower $^{13}C$ discrimination in the photosynthetic process and, hence, higher $^{13}C$ values in plant tissues (Farquhar & Richards, 1984; Saurer *et al.*, 2004).

In November 2003, 10 cm long wood cores were taken from 10 co-dominant trees of each stand and pooled for analysis. These stands ranged between 7 and 10 years of age and had 800–1000 trees $ha^{-1}$. Four cores were taken at breast height from each cardinal direction, dried to constant mass at 65 °C and ground. $^{13}C/^{12}C$ ratios were determined by mass spectrometry (Finnigan MAT Delta Plus XL, Bremen, Germany) on the $CO_2$ produced by combusted samples and expressed as $\delta^{13}C$ values.

*Stream chloride concentration*

In order to explore grassland afforestation effects at the catchment scale, and to provide an independent measure of water use, we analyzed chloride concentration data from streams draining catchments with different proportions of afforestation within and close to the study region. Since chlorine is not present in most rocks (Bowen, 1966) and is not significantly accumulated in plant biomass (Epstein, 1972), choride ion inputs from precipitation should balance outputs in streamflow (Vitousek, 1977). Under this assumption, differences in stream chloride concentration should represent a relative measure of catchment ET (Hedin *et al.*, 1995). Chloride concentration data were obtained from a previous survey (Auge & Santi, 2002) of 18 small streams with similar parent material and slopes. The area of their watershed varied between 21 and 328 $km^2$ and afforested proportion ranged from $<0.05\%$ to 17.8%.

*Statistical analysis*

Statistical analyses were conducted using SAS 8.02. The effects of land use and soil type on ET, FPAR, and albedo were assessed using GLM-ANOVA procedures. We explored the relationships between rainfall–open pan evaporation water balances and ET using linear and saturation response models. We also compared the stability of ET through time, computing the interdate coefficient of variation (CV). Productivity and $\delta^{13}C$ values were also analyzed using GLM-ANOVA. Multiple comparisons were assessed following Duncan tests.

## Results

*Grassland-plantations contrasts*

In spite of having lower albedo, and hence higher net radiation inputs, tree plantations sustained lower canopy temperatures than native grasslands, which indicated higher evaporative water losses for this

**Table 1** Radiometric, thermal, and evaporative characteristics of *Eucalyptus grandis* plantations and native grasslands across soil types

| | | NDVI | | $T_s - T_{a50\,m}$(°C) | | Albedo | | FPAR (%) | | ET (mm day$^{-1}$) | |
|---|---|---|---|---|---|---|---|---|---|---|---|
| | *n* | Mean | SE | Mean | SE | Mean | SE | Mean | SE | Mean | SE |
| *Tree plantations* | | | | | | | | | | | |
| Fine | 11 | 0.754 a | 0.01 | 3.22 b | 1.07 | 0.163 de | 0.003 | 90.8 a | 1.5 | 3.02 b | 0.32 |
| Medium | 33 | 0.765 a | 0.01 | 2.79 bc | 0.58 | 0.166 cd | 0.002 | 91.7 a | 0.9 | 3.15 b | 0.19 |
| Coarse | 8 | 0.759 a | 0.02 | 2.29 cd | 1.10 | 0.158 e | 0.003 | 91.2 a | 2.0 | 3.38 a | 0.40 |
| Coastal | 7 | 0.760 a | 0.02 | 1.89 d | 1.04 | 0.159 de | 0.002 | 91.5 a | 2.1 | 3.50 a | 0.48 |
| Mean | | 0.760 | | 2.67 | | 0.163 | | 91.4 | | 3.22 | |
| *Grasslands* | | | | | | | | | | | |
| Fine | 10 | 0.585 bc | 0.03 | 7.78 a | 1.28 | 0.183 a | 0.004 | 70.6 bc | 4.0 | 1.74 c | 0.25 |
| Medium | 28 | 0.588 bc | 0.02 | 7.90 a | 0.87 | 0.178 ab | 0.002 | 71.0 bc | 2.3 | 1.75 c | 0.16 |
| Coarse | 10 | 0.590 b | 0.04 | 7.92 a | 1.49 | 0.175 b | 0.004 | 71.2 b | 4.4 | 1.77 c | 0.25 |
| Coastal | 10 | 0.569 c | 0.04 | 7.62 a | 1.40 | 0.172 bc | 0.006 | 68.7 c | 4.4 | 1.90 c | 0.30 |
| Mean | | 0.584 | | 7.82 | | 0.177 | | 70.5 | | 1.78 | |

Mean and standard error (SE) of normalized difference vegetation index (NDVI), temperature difference ($T_s - T_{a50\,m}$), albedo, fraction of photosynthetically active radiation intercepted by green vegetation (FPAR) and actual evapotranspiration rate (ET) computed from Landsat images for tree plantations and grasslands. The mean values were obtained by averaging the seven dates analyzed. Both covers are discriminated by soil textural types. Coastal plots were located $<1000$ m away from the shores of the Salto Grande reservoir and Uruguay River. Letters show significant differences ($P<0.05$) among all combination of vegetation $\times$ soil type (Duncan's test). The number of plots is indicated (*n*).

vegetation type across the whole textural gradient and throughout all the dates that we explored (Table 1). On average, tree plantations used $\sim 81\%$ more water than grasses with absolute ET differences ranging between 1.87 mm day$^{-1}$ (12/26/2002) and 0.97 mm day$^{-1}$ (07/19/2002) (Fig. 2a). Tree plantations maintained their canopies $\sim 5\,^{\circ}$C cooler than grasslands ($P<0.0001$) in spite of receiving $\sim 3\%$ higher net energy inputs as a result of their lower albedo (Table 1). The largest absolute departure of surface temperature from air temperature was observed on the driest date (11/18/2000) in both vegetation types.

Tree plantations intercepted a higher proportion of photosynthetically active radiation than grasslands, as suggested by their consistently higher NDVI values (Table 1, $P<0.0001$). Tree plantations showed higher and more stable NDVI values than grasslands at all sites and throughout all dates (absolute minimum and maximum NDVI = 0.63 and 0.85 for tree plantations and 0.28 and 0.75 for grasslands, respectively) (Fig. 2b). In association with these NDVI contrasts, the fraction of PAR intercepted (FPAR) by canopies on nonwinter and winter dates averaged 94% and 85% for tree plantations and 77% and 53% for grasslands, respectively.

### *Temporal changes in ET and climate*

In agreement with our prediction, ET was more stable through time in tree plantations than in grasslands (Fig. 3). The coefficient of variation of ET across dates was significantly lower in plantations compared with grasslands (36.5% and 49.2%, respectively; $P<0.0001$) (Fig. 3b). When we compared ET values on two dates with similar net radiation (11/18/2000 = 14.2 MJ m$^{-2}$ day$^{-1}$ and 02/06/2001 = 12.7 MJ m$^{-2}$ day$^{-1}$) but highly different water availability, as indicated by the rainfall–open pan evaporation water balance of the 18 previous days (11/18/2000 = $-24.5$ mm and 02/06/2001 = $+3.6$ mm, Fig. 2c), we found that tree plantation and grassland ET responded differently. While plantation ET increased $\sim 40\%$, in grasslands, ET rates were doubled. It is important to note that these ET contrasts occurred with slight to nil NDVI changes between both dates (tree plantations = $+2.5\%$; grasslands = $+1.7\%$).

Changes in tree plantation and grassland ET across dates were best explained by the climatic water balance of the previous 15–20 days (Figs 4a and b). The relative degree by which potential ET was met by actual ET, characterized by the ratio between ET and open pan evaporation (ET/OPE), became increasingly correlated with water balance, measured as the difference between rainfall and open pan evaporation, when the previous 15–20 days were considered. Longer or shorter periods of water balance integration showed poorer and non-significant correlations (Figs 4a and b). It is interesting to note that between $-25$ and $+10$ mm of water balance, tree plantation and grassland ET presented a similar response, with slopes being not statistically

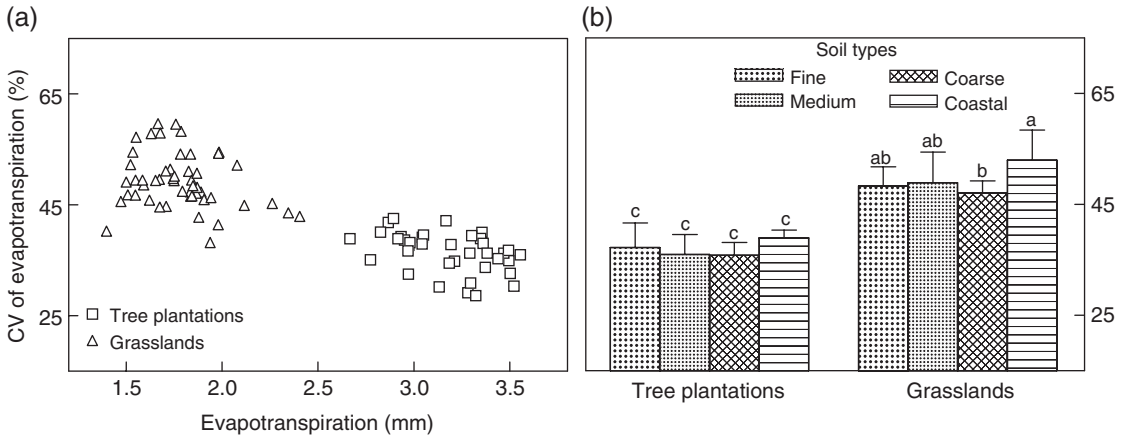


**Fig. 3** Temporal variability of evapotranspiration (ET) in *Eucalyptus grandis* plantations and native grasslands. Relationship between mean ET and coefficient of variation (CV) of ET across dates for 59 and 58 individual plantation and grassland plots, respectively (a). The average CV of evapotranspiration in plantations and grasslands is shown for different soils types (b). Letters show significant differences ($P < 0.05$) among all combinations of vegetation × soil type (ANOVA). Bars correspond to standard deviation.

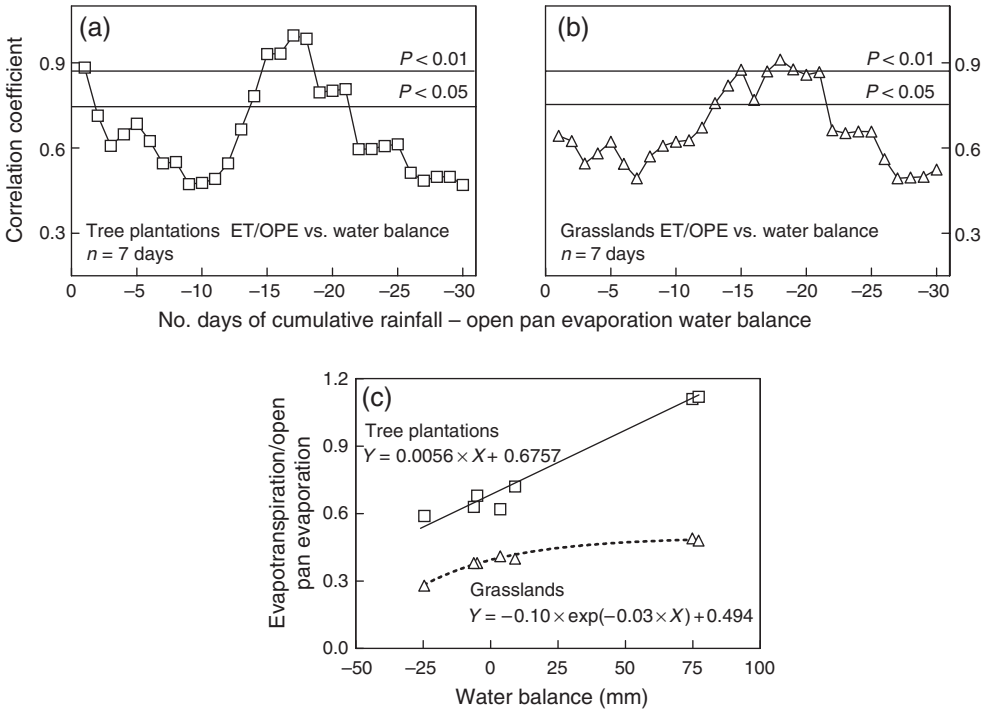


**Fig. 4** Evapotranspiration in *Eucalyptus grandis* plantations and native grasslands in relation to water balance. Associations between daily evapotranspiration (ET)/open pan evaporation (ET/OPE) of tree plantations (a) and grasslands (b) and cumulative water balance considering 1–30 days prior to the image acquisition date. Response of ET/OPE values to the water balance of the 18 previous days (c). Linear models were evaluated in both vegetation types and improved by a saturation response model in grasslands. Water balances were computed as rainfall–open pan evaporation (WB = R–OPE). Correlation levels that correspond to significance levels of $P < 0.05$ and $P < 0.01$ are indicated with horizontal lines.

different from each other, but at higher rainfall inputs both responses differed and the curves separated (Fig. 4c). While plantation ET continued increasing, grassland ET plateauing at + 75 mm of water balance and the use of a saturation response model resulted in a better fit than the linear one suggesting that other constraints rather than rainfall inputs are limiting grasses ET.

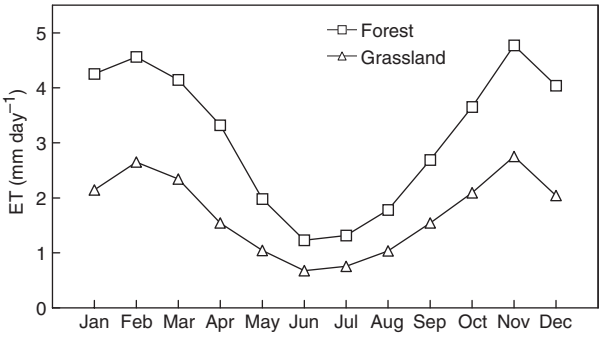


**Fig. 5** Seasonal evapotranspiration (ET) patterns for *Eucalyptus grandis* plantations and native grasslands. Mean monthly values were computed using regression (forests) and saturation models (grasslands) that link ET to water balance and monthly statistics of open pan evaporation and rainfall for the study region.

Using the previous relationships and historical monthly precipitation and pan evaporation data we were able to integrate ET at the monthly and annual scale (Fig. 5). Maximum ET values were estimated for November (tree plantations = 4.77 mm day$^{-1}$; grassland = 2.75 mm day$^{-1}$) and minimum values for June (tree plantations = 1.23 mm day$^{-1}$; grassland = 0.67 mm day$^{-1}$). Maximum differences between both covers seem to be achieved in January. Integrating to annual scale, we obtained mean ET values of 627 and 1148 mm yr$^{-1}$ for grasslands and tree plantations, respectively.

### *Sensitivity analysis and validation*

Assuming equal $B$ values for forests and grasslands (an underestimation of heat loss capacity in forest canopies) increased ET differences between tree plantations and grasslands on both dates analyzed (1.67–2.25 mm day$^{-1}$ on 11/18/2000; 1.43–1.67 mm day$^{-1}$ on 02/06/2001; Fig. 6). An increment of $B_{\text{forest}}$ of +25% decreased differences between both covers (1.67–0.94 mm day$^{-1}$ on 11/18/2000; 1.43–1.12 mm day$^{-1}$ on 02/06/2001). It is interesting to note that even using the highest $B_{\text{forest}}$ value reported in the literature (Sanchez & Caselles, 2004), tree plantations maintained higher ET values than grasslands. ET values could have been similar for both vegetation types only with $B_{\text{forest}}$ values as high as 0.90–1.2, very unlikely values for any vegetation type (Carlson *et al*., 1995). Varying $T_s \pm 1$ K in both types of vegetation led to small changes in ET contrasts between both covers on 06/02/2001 and negligible changes on 11/18/2000. On 06/02/2001 increasing $T_s$ decreased ET differences (1.43–1.38 mm day$^{-1}$) between plantations and grasslands; by contrast, decreasing $T_s$ increased ET differences (1.43–1.51 mm day$^{-1}$) (Fig. 6).

Transpiration rates derived from sap flux measurements averaged 2.7 mm day$^{-1}$ (range 1.55–5.4 mm day$^{-1}$) for the period of 12–22 December 2003. The ratio transpiration/open pan evaporation averaged 0.58 and showed a good agreement with the average ET/OPE value of December (0.52) derived from satellite estimates. The maximum daily ET computed from satellite images (5.45 mm day$^{-1}$) matched our sap flux measurements.

### *ET and soil texture*

ET changed with soil texture in tree plantations and grasslands but, in contrast with our prediction, did not peak in medium textured soils for any vegetation type (Table 1). The ranking of ET values for tree plantations across soil types was coastal > coarse > medium > fine and maintained throughout all dates with the exception of the most humid date, when ET peaked in coarse textured soils. These site differences expanded during the driest date (11/18/2000), when tree plantations on coastal sites used 25% and 17% more water than those located on fine and medium textured, respectively. On a more humid date (02/06/2001) these differences declined to 8% and 10%, respectively. These contrasts suggest a higher water availability to trees in coastal soils that manifests more strongly on ET patterns during drier periods. ET differences across grassland sites were not significant when all dates were averaged, but were expressed when they were analyzed independently. On the driest date (11/18/2000) grasslands had highest ET values on fine textured soils, whereas on more humid dates they either had no differences or they peaked in coastal sites (12/26/02 and 01/27/03) ($P < 0.05$).

The effect of texture on FPAR was less pronounced than on ET (Table 1). No differences in tree plantation FPAR were observed across soil types when all dates were averaged ($P = 0.25$), although higher FPAR was observed on tree plantations located in fine textured soils on the most humid date (07/19/2002). In grasslands, coastal sites displayed the lowest FPAR values across all dates with the exception of 6 February and 11 April when the lowest values were observed in fine textured soils ($P < 0.05$). On 18 November, FPAR followed the same trend as ET and peaked in fine textured soils.

### *Water limitation and soil texture*

The composition of stable isotopes of carbon in tree stems indicated that water use efficiency was maximum in plantations located in medium textured soils, where productivity peaked, and lower in coarser and finer soils, where productivity was 33–50% lower (Table 2). If water availability was causing production declines in fine and coarse textured soils (hypothesis 3A), we

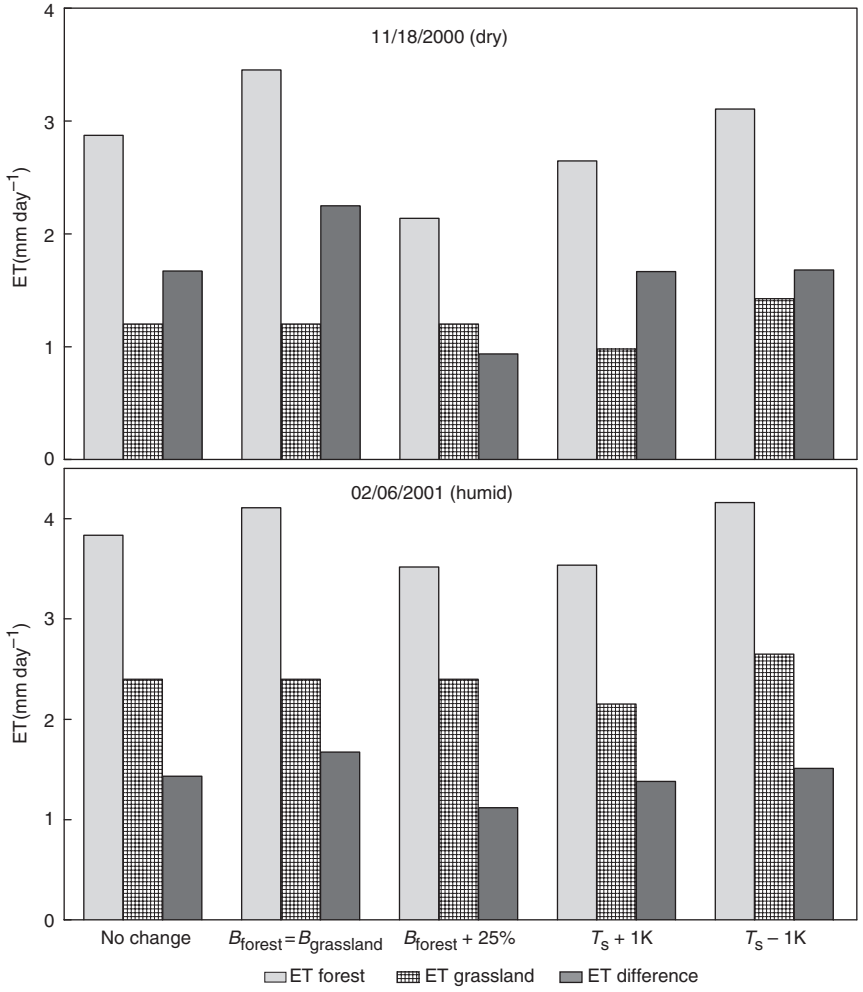


**Fig. 6** Sensitivity of evapotranspiration (ET) estimates to variations in $B_{forest}$ parameter ($B_{forest} = B_{grassland}$ in the low end and a raise of 25% in the high end) and surface temperature ($T_s$, $\pm$ 1 K). Two dates with different water availability conditions were evaluated (11/18/2000-dry- and 02/06/2001-humid-). Mean ET values for tree plantation and grassland stands, as well as their absolute differences are shown.

**Table 2** Productivity and $\delta^{13}C$ wood values of *Eucalyptus grandis* plantations across the soil textural gradient of the study region (mean and standard error)

| | Productivity ($m^3\,ha^{-1}\,yr^{-1}$) | | | $\delta^{13}C$ wood (‰) | | |
|---|---|---|---|---|---|---|
| | Mean | *n* | SE | Mean | *n* | SE |
| Fine | 26.7 c | 13 | 0.27 | −28.11 b | 4 | 0.14 |
| Medium | 53.9 a | 14 | 0.52 | −27.51 a | 5 | 0.08 |
| Coarse | 35.8 b | 13 | 0.43 | −28.15 b | 5 | 0.08 |

Productivity values were obtained from previous local studies and $\delta^{13}C$ values were assessed from wood samples taken at breast height in November 2003. Letters indicate significant differences for productivity ($P < 0.01$) and $\delta^{13}C$ ($P < 0.1$) based on Duncan's tests. The number of plots is indicated (*n*).

should have found highest water use efficiency in these soils. The opposite pattern was observed (Table 2), supporting the idea that other resources or factors constrain productivity in these soils (hypothesis 3B). In agreement with the isotopes analysis, ET rates computed from Landsat images (higher in coarse and similar in medium and fine textured soils; Table 1) indicated that water limitation was not the cause of forest productivity decline in extreme textures.

### *ET and plantation age*

ET rates and PAR interception by tree plantations increased rapidly after planting, exceeding grasslands in less than 3 years (Fig. 7). At 0–1 years of age, tree plantations intercepted $\sim$ 34% less radiation and used

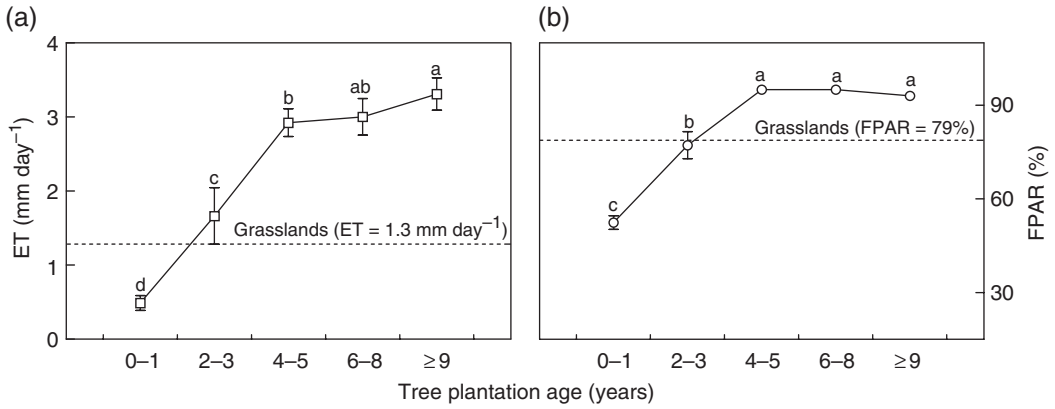


**Fig. 7** Changes in daily evapotranspiration (ET) (a) and fraction of photosynthetically active radiation intercepted (b) with tree plantation age. All values were computed from the 18 November 2000 image in plots located on medium textured soils. Letters show significant differences ($P<0.05$) among age classes. Mean ET and FPAR values of grasslands in the same soils are indicated with horizontal lines. $N = 3$, 4, 9, 6, 9 for age classes of 0–1, 2–3, 4–5, 6–8, $\geq 9$ years and 28 for grasslands. Bars correspond to standard deviation.

$\sim 62\%$ less water than grasslands ($P<0.05$), while at the next stage (2–3 years) both types of vegetation intercepted similar amount of radiation, but tree plantations used $\sim 28\%$ more water ($P<0.05$). It is important to note that ET and FPAR patterns differed as plantations got older. While FPAR rose until 4–5 years of age and then became steady, ET continued increasing until the harvest time (Fig. 7), suggesting a lower water use efficiency in older plantations.

*Independent estimates of water use*

In order to obtain independent evidence about grassland and tree plantation ET patterns, we made use of stream chloride concentration data and modeling at catchment scale. We found a positive and linear association between the percent of catchment afforested and stream chloride concentration (Fig. 8; $r^2 = 0.46$, $P<0.01$). Levels of $Cl^-$ varied more than four-fold among watershed streams. Afforesting 20% of the catchment tripled $Cl^-$ concentration (4.2 mg L$^{-1}$ for nonafforested vs. 12.8 mg L$^{-1}$ for 20% afforested). If we assumed that $Cl^-$ acts as a conservative tracer of water movement, this regression analysis would indicate decreasing water yield and, thus, higher evaporative water losses, as afforested area increases. Using a simple two-parameter model to estimate mean annual ET at the catchment scale (Zhang *et al.*, 2001), we obtained mean values of 721 and 1031 mm yr$^{-1}$ for the nonafforested and the fully afforested watershed, respectively. Differences between satellite and modeled estimates of ET were 116 mm ( + 11.3%) for plantations and 95 mm (−13.1%) for grasslands.

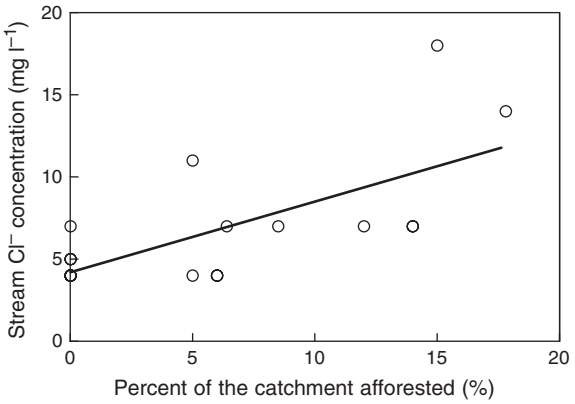


**Fig. 8** Stream chloride concentration (mg L$^{-1}$) as a function of the proportion (%) of the catchment area that is afforested. Stream chloride data were obtained from a previous survey (Auge & Santi, 2002) and total and afforested catchment area was measured using Landsat images and topographic maps.

## Discussion

Tree plantations used consistently more water than grasslands across soil types during both dry and wet periods, suggesting an almost twofold raise of evaporative water losses in afforested areas (Fig. 2). These ET contrasts matched observations from other afforested grasslands of the world (Greenwood *et al.*, 1985; Hodnett *et al.*, 1995; Scott *et al.*, 2000; Zhang *et al.*, 2001) and evidenced that the greater evaporative water loss in tree plantations was likely caused by an enhancement of atmosphere–canopy coupling and better access to moisture sources following the establishment of trees. The higher aerodynamic conductance (Kelliher *et al.*, 1993)

and more effective capture of advective energy (Calder, 1998) of tree canopies compared with grasslands probably explain the different responses of both types of vegetation to increasing rainfall inputs (Fig. 4c). As grasses are short, they are less able to drive inputs of advected energy (Calder, 1998), so they are solar radiation dependent, especially under wet conditions. The low leaf area of grasses, sustained mainly by grazing, could also limit ET because of a reduced canopy conductance (Kelliher *et al*., 1993). Mirroring our results, catchments studies show increasing ET differences between grasslands and forests as annual rainfall increases (Zhang *et al*., 2001). Additionally, the deeper root system that trees, and particularly eucalyptus, are likely to possess (Canadell *et al*., 1996; Dye *et al*., 1997) probably warranted a sustained water supply explaining more stable ET patterns in tree plantations (Fig. 3b). Long-term analyses of annual ET in several biomes around the world have also exhibited higher temporal variation in nonforested ecosystems (Frank & Inouye, 1994).

ET shifts with soil texture were nil in grasslands but significant in tree plantations (Table 1). In contrast with our initial expectation, ET did not peak in medium textured soils (with probably highest soil water availability) but remained unaffected by soil texture in grasslands and increased as texture became coarser in tree plantations. Differences in groundwater availability rather than water-holding capacity are likely to cause these patterns across the soil gradient. Sustained groundwater use requires access of roots to the water table or capillary fringe and sediments with sufficiently high saturated hydraulic conductivity that can convey groundwater to roots at rates that match water requirements by tree canopies (Jobbagy & Jackson, 2004). These requirements are more likely to be met on coarse sediments in which saturated conductivity is high and in coastal positions where the water tables are shallow, in agreement with our observations. Two indicators of groundwater uptake by plants, diurnal water table fluctuations and groundwater salinization (Johansson, 1986; Heuperman, 1999; Sapanov, 2000) suggested that *E. grandis* plantations use groundwater in coarse textured soils. Detailed continuous measurements of groundwater level in an *E. grandis* plantation on coarse textured soils manifested diurnal fluctuations of $\sim 2$ cm between night highs and midday lows (M. Nosetto and N. Tesón, unpublished data). Direct measurements of groundwater electric conductivity at two coastal plantations with water tables at $\sim 2.5$ m of depth showed values $>20$ times higher than in the local groundwater source at the Salto Grande reservoir (data not shown). Throughout the study region water tables were probably shallow enough ($<25$ m) to be accessed by the deep roots of Eucalyptus ($\sim 28$ m *E. grandis*; Dye *et al*., 1997); however, the low conductivity of clay-textured sediments could have prevented lateral groundwater transfer towards tree roots in fine and perhaps medium textured soils. Further experiments are needed to confirm this possibility.

We hypothesized that the productivity declines of tree plantations observed from medium textured soils towards fine and coarse textured ones were caused by (A) a water limitation, or alternatively by (B) nonwater-related constraints. Our ET estimates together with the carbon isotopes composition of tree stems and the productivity records support the second alternative (Tables 1 and 2). Lower water use efficiency in plantations located on soils of extreme texture points to nonwater-related constraints in those situations. Nutrient limitation and poor oxygen supply to roots could be the main constraints to tree growth in coarse and fine textured soils, respectively. A deficient nutrient supply in coarse textured soils compared with medium ones can be inferred from their contrasting soil organic matter contents ($\sim 0.5\%$ vs. $\sim 3.3\%$; INTA 1993) and cation exchange capacities ($\sim 1.2$ vs. $\sim 12$ m.e./100 g; INTA, 1993). Large responses of eucalyptus plantations productivity to the use of fertilizer (Dalla Tea, 1993) also suggest that soil nutrition is a key determinant of trees performance on coarse-textured soils of the study region. Considering *E. grandis* sensitivity to poorly drained soils (Henri, 2001) we speculate that this feature could be restricting forest productivity in fine textured soils. The adverse effect of clay content in the growth of trees has been previously suggested through a positive relationship between aboveground forest productivity and depth to the clay layer (Sepliarsky & Dalla Tea, 1993). Iron and manganese concretions observed along profiles of fine textured soils (INTA, 1993) indicate periods of low oxygen potential, which could in turn negatively affect the growth of trees. Our analysis suggests that, if water is not constraining productivity in coarse and fine textured soils, making up for nutrient and oxygen limitations using fertilizer and anoxic resistant species, for instance, could result in not only higher productivity rates but also higher evaporative water losses.

ET changes with tree plantation age showed that forests used more water than grasslands as early as 2–3 years after planting and rose at a steady state until 4–5 years of age, having a slow increase afterwards (Fig. 7). This is particularly important considering that almost 85% of the afforested plots of the region are more than 3 years of age (SAGPyA, 2002), and evidences the strong impact of afforestation in the evaporative water losses of the landscape as a whole. Another interesting feature emerging from the analysis of plantation age is that while ET rates maintained slight increases after 4–5

years of age, the intercepted radiation stabilized or even decreased after that age, suggesting a decline of water use efficiency. This FPAR pattern parallels well independent estimates of growth of biomass in the same area (Marcó, 1988b; Frangi *et al*., 2000) and confirms the general age-related decline in forest productivity for these plantations (Assmann, 1970; Forrest & Ovington, 1970; Binkley *et al*., 2002). As water use by trees did not decrease as trees got older, on the contrary it increased, our results suggest that the growth decline of these plantations is not related to an increased hydraulic resistance (Ryan *et al*., 1997). Therefore, other explanations, such as diminished nutrient supply (Binkley *et al*., 1995; Schulze *et al*., 1995) or competition-related changes in stand structure (Binkley *et al*., 2002), are more likely to happen. It is interesting to highlight at this point that keeping tree plantations young through short rotations, as it is required to have high economic yields, instead of letting them age, would result in little or no change in water balances as it has been proposed for other regions (Vertessy *et al*., 2001).

What would the effects of more massive afforestation on the regional hydrological cycle be? Argentina and Uruguay have $\sim 37$ millions of hectares suitable for afforestation but only $\sim 4\%$ of this area is currently occupied by tree plantations (SAGPyA, 1999; Arrate, 2000). Taking into account current governmental subsidies for tree planting and the prospective carbon sequestration market (IGBP TCWG, 1998; Wright *et al*., 2000), an expansion of the forested area is highly possible. Beneficial and problematic changes could stem from the higher evaporative water losses of tree plantations. While significant flood and erosion control associated with reduced runoff and streamflow are feasible positive effects (Scott & Lesch, 1997), water yield and groundwater recharge reduction are likely negative consequences of afforestation in grasslands (Bosch & Hewlett, 1982; Heuperman, 1999). In our study region, average percent of catchment afforestation reaches $\sim 10\%$. If this value was to reach 50% (something common in other heavily afforested regions of the world) water yield would be reduced to less than 2/3 of its original value (462 vs. $723\,\mathrm{mm\,yr^{-1}}$). In addition to changes in water quantity, grassland afforestation could also modify water chemistry through changes in the circulation of elements (Jobbágy & Jackson, 2003).

As current climate and vegetation are in a dynamic equilibrium dictated by their reciprocal influences (Nobre, 1991), deep land-use changes, like the one studied here, may affect regional climate. Model simulations of forests to grasslands conversion in Amazonian ecosystems have predicted increased surface temperature, lower ET, and declining precipitation (Lean & Warrilow, 1989; Shukla *et al*., 1990). Observations in the Amazon basin suggest that above a threshold of 20% of deforestation cloud cover starts showing significant changes (Durieux *et al*., 2003). Whether massive grassland afforestation will mirror this climate shift is still uncertain, but is possible according to our results. Issues of scale, distribution of the afforested patches, and wind patterns will probably be crucial in this process.

## Acknowledgements

We wish to thank Carlos di Bella and Gervasio Piñeiro for their insightful comments and suggestions for this work. Diana Diaz, Natalia Tesón, and Lorena Grion assisted us in the field and lab work. Special thanks to Rob Jackson for helpful comments and collaboration at the initiation of the project and the use of mass spectrometry facilities at Duke University. Landsat images were provided by CONAE (Argentina) and meteorological data by INTA (Concordia, Argentina). This work was funded by Fundación Antorchas (Career Start up) and Inter-American Institute for Global Change Research (IAI-SGP 004). Marcelo Nosetto was supported by CONICET (Argentina–Beca Doctoral Interna) and a fellowship from IAI.

## References

Arrate CP (2000) Uruguay's destructive plantation model. *Seedling*, **17**, 14–22.

Assmann E (1970) *The Principles of Forest Yield Study*. Pergamon Press, Oxford.

Auge M, Santi M (2002) *Disponibilidad de agua subterránea para la producción arrocera de la provincia de Entre Ríos: Inventario a nivel de reconocimiento,* Consejo Federal de Inversiones, Buenos Aires, 209 pp.

Binkley D, Smith FW, Son Y (1995) Nutrient supply and declines in leaf area and production in lodgepole pine. *Canadian Journal of Forest Research*, **25**, 621–628.

Binkley D, Stape JL, Ryan MG *et al*. (2002) Age-related decline in forest ecosystem growth: an individual-tree, stand-structure hypothesis. *Ecosystems*, **5**, 58–67.

Bosch JM, Hewlett JD (1982) A review of catchment experiments to determine the effect of vegetation changes on water yield and evapotranspiration. *Journal of Hydrology*, **55**, 3–23.

Bowen HJM (1966) *Trace Elements in Biochemistry*. Academic Press, London.

Brasa Ramos A, Martín de Santa Olalla F, Caselles V (1996) Maximum and actual evapotranspiration for barley (*Hordeum vulgare* L.) through NOAA satellite images in Castilla-La Mancha, Spain. *Journal of Agricultural Engineering Research*, **63**, 283–294.

Brizuela A, Milera S, Mestres J (2003) *Plantaciones de Eucaliptos y Pinos en los departamentos del este de Entre Ríos*. XVIII Jornadas Forestales de Entre Ríos, Concordia, Argentina.

Brutsaert W (1986) Catchment-scale evaporation and atmospheric boundary layer. *Water Resources Research*, **22**, 39–46.

Calder IR (1998) Water use by forests, limits and controls. *Tree Physiology*, **18**, 625–631.

Calder IR, Hall MJ, Prasanna KT (1993) Hydrological impact of *Eucalyptus* plantation in India. *Journal of Hydrology*, **150**, 635–648.

Calder IR, Rosier PTW, Prasanna KT *et al*. (1997) *Eucalyptus* water use greater than rainfall input – a possible explanation from southern India. *Hydrology and Earth System Science*, **1**, 249–256.

Campbell GS, Norman JM (1998) *An Introduction to Environmental Biophysics*. Springer-Verlag, New York.

Canadell J, Jackson RB, Ehleringer JR *et al*. (1996) Maximum rooting depth of vegetation types at the global scale. *Oecologia*, **108**, 583–595.

Carlson T, Capehart W, Gillies R (1995) A new look at the simplified method for remote sensing of daily evapotranspiration. *Remote Sensing of Environment*, **54**, 161–167.

Carlson TN, Buffum MJ (1989) On estimating total daily evapotranspiration from remote surface temperatures measurements. *Remote Sensing of Environment*, **29**, 197–207.

Caselles V, Artigao MM, Hurtado E *et al*. (1998) Mapping actual evapotranspiration by combining Landsat TM and NOAA-AVHRR images: application to the Barrax Area, Albacete, Spain. *Remote Sensing of Environment*, **63**, 1–10.

Chavez PS Jr. (1989) Radiometric calibration of Landsat Thematic Mapper multispectral images. *Photogrammetric Engineering and Remote Sensing*, **55**, 1285–1294.

Choudhury BJ (1987) Relationships between vegetation indices, radiation absorption, and net photosynthesis evaluated by a sensitivity analysis. *Remote Sensing of Environment*, **22**, 209–233.

Dalla Tea F (1993) *Evaluación temprana de herbicidas y fertilizantes en plantaciones de Eucalyptus grandis*. Congreso Forestal Argentino y Latinoamericano, Paraná, Argentina.

Durieux L, Machado LAT, Laurent H (2003) The impact of deforestation on cloud cover over the Amazon arc of deforestation. *Remote Sensing of Environment*, **86**, 132–140.

Dye PJ, Poulter AG, Soko S *et al*. (1997) *The determination of the relationship between transpiration rate and declining available water for Eucalyptus grandis*, Water Research Commission.

Eastman RJ (1999) *IDRISI 32 Guide to GIS and Image Proccessing*. Clark Labs, Worcester.

Epstein E (1972) *Mineral Nutrition of Plants: Principles and Perspectives*. Wiley and Sons, New York.

FAO (2001) *Proyecto Regional GCP/RLA/133/EC 'Información y análisis para el manejo forestal sostenible'*. Recursos forestales y cambio en el uso de la tierra en el Uruguay, Santiago de Chile, Chile.

Farquhar GD, O'Leary HO, Berry JA (1982) On the relationship between carbon isotope discrimination and the intercellular carbon dioxide concentration in leaves. *Australian Journal of Plant Physiology*, **9**, 121–137.

Farquhar GD, Richards RA (1984) Isotopic composition of plant carbon correlates with water use efficiency of wheat genotypes. *Australian Journal of Plant Physiology*, **11**, 539–552.

Forrest WG, Ovington JD (1970) Organic matter changes in an age series of *Pinus radiata* plantations. *Journal of Applied Ecology*, **7**, 177–186.

Frangi JL, Goya JF, Bianchini F *et al*. (2000) *Ciclo de nutrientes en plantaciones de Eucalyptus grandis (Hill ex Maiden) de distintas edades en la provincia de Entre Ríos*, SAGPyA-BIRF, Concordia. Entre Ríos.

Frank DA, Inouye RS (1994) Temporal variation in actual evapotranspiration of terrestrial ecosystems: patterns and ecological implications. *Journal of Biogeography*, **21**, 401–411.

Geary TF (2001) Afforestation in Uruguay – study of a changing landscape. *Journal of Forestry*, **99**, 35–39.

Goya JF, Frangi JL, Dalla Tea F (1997) Relación entre biomasa aérea, área foliar y tipos de suelos en plantaciones de *Eucalyptus grandis* del NE de Entre Ríos, Argentina. *Revista de la Facultad de Agronomía, La Plata*, **102**, 11–21.

Granger R, Gray DM (1990) A net radiation model for calculating daily snowmelt in open environments. *Nordic Hydrology*, **21**, 217–234.

Granier A (1985) Une nouvelle methode pour la mesure du flux de seve brute dans le tronc des arbres. *Annales des Sciences Forestieres*, **42**, 81–88.

Granier A (1987) Evaluation of transpiration in a Douglas-fir stand by means of sap flow measurements. *Tree Physiology*, **3**, 309–320.

Greenwood EAN, Klein L, Beresford JD *et al*. (1985) Differences in annual evaporation between grazed pasture and *Eucalyptus* species in plantations on a saline farm catchment. *Journal of Hydrology*, **78**, 261–278.

Hedin LO, Armesto J, Johnson J *et al*. (1995) Patterns of nutrient loss from unpolluted, old-growth temperate forests: evaluation of biogeochemical theory. *Ecology*, **76**, 493–509.

Henri CJ (2001) Soil-site productivity of *Gmelina arborea, Eucalyptus urophylla* and *Eucalyptus grandis* forest plantations in western Venezuela. *Forest Ecology and Management*, **144**, 255–264.

Heuperman A (1999) Hydraulic gradient reversal by trees in shallow water table areas and repercussions for the sustainability of tree-growing systems. *Agricultural Water Management*, **39**, 153–167.

Hillel D (1998) *Environmental Soil Physics*. Academic Press, San Diego.

Hodnett MG, da Silva LP, da Rocha HR *et al*. (1995) Seasonal soil water storage changes beneath central Amazonian rainforest and pasture. *Journal of Hydrology*, **170**, 233–254.

Horton RE (1919) Rainfall interception. *Monthly Weather Review*, **47**, 603–623.

Hurtado E, Caselles V, Artigao MM (1994) *Mapping actual evapotranspiration by combining Landsat TM and NOAA-AVHRR images in the Albacete region*, Spain. Image Quality and Interpretation for Mapping,, NA PG Grignon, RSS-SFPT, 1–3 September, pp. 29–32.

IGBP TCWG. (1998) The terrestrial carbon cycle: implications for the Kyoto Protocol. *Science*, **280**, 1393–1394.

Inoue Y, Moran MS (1997) A simplified method for remote sensing of daily canopy transpiration – a case study with direct measurements of canopy transpiration in soybean canopies. *International Journal of Remote Sensing*, **18**, 139–152.

INTA (1984) *Plan Mapa de Suelos de la Provincia de Entre Ríos. Convenio INTA-Gobierno de Entre Ríos*. Suelos y erosión de la provincia de Entre Ríos, INTA-EEA,Paraná.

INTA (1993) *Carta de Suelos de la República Argentina*. Departamento Concordia, Entre Ríos.

INTA (1995) *Manual para productores de Eucaliptos de la Mesopotamia Argentina*.

Irish RR (2000) *Landsat 7 science data user's handbook*. Report 430-15-01-003-0, National Aeronautics and Space Administration.

Jackson RD, Reginato RJ, Idso SB (1977) Wheat canopy temperature: a practical tool for evaluating water requirements. *Water Resources Research*, **13**, 651–656.

Jobbagy EG, Jackson RB (2003) Patterns and mechanisms of soil acidification in the conversion of grasslands to forests. *Biogeochemistry*, **64**, 205–229.

Jobbagy EG, Jackson RB (2004) Groundwater use and salinization with grassland afforestation. *Global Change Biology*, **10**, 1299–1312.

Johansson PO (1986) Diurnal groundwater level fluctuations in sandy till – a model analysis. *Journal of Hydrology*, **87**, 125–134.

Kelliher FM, Leuning R, Schulze ED (1993) Evaporation and canopy characteristics of coniferous forests and grasslands. *Oecologia*, **95**, 153–163.

Lagouarde JP, Brunet Y (1989) Spatial integration of surface latent heat flux and evaporation mapping. *Advances in Space Research*, **9**, 259–264.

Landi M, Oesterheld M, Deregibus VA (1987) *Manual de especies forrajeras de los pastizales naturales de Entre Ríos*. AACREA.

Lean J, Warrilow DA (1989) Climatic impact of Amazon deforestation. *Nature*, **342**, 411–413.

Liang S (2000) Narrowband to broadband conversions of land surface albedo. I Algorithms. *Remote Sensing of Environment*, **76**, 213–238.

Marcó MA (1988a) *Crecimiento del Eucalyptus grandis en diferentes suelos de Concordia. Resultados a los 10.5 años*. VI Congreso Forestal Argentino, pp. 510–511, Santiago del Estero, Argentina.

Marcó MA (1988b) *Incidencia del origen de la semilla y el sitio en el crecimiento de Eucalyptus grandis en el Nordeste de Entre Ríos*. III Jornadas Forestales de Entre Ríos, Concordia, Argentina.

Monteith JL (1988) Does transpiration limit the growth of vegetation or vice versa? *Journal of Hydrology*, **100**, 57–68.

Nobre CA (1991) Possible climatic impacts of amazonia deforestation. In: *Water Management of the Amazon Basin* (eds Braga BP, Fernández-Jáuregui CA), Montevideo, Uruguay.

Noy-Meier I (1973) Desert ecosystems: environment and producers. *Annual Review of Ecology and Systematics*, **4**, 25–51.

Qin Z, Karnieli A, Berliner P (2001) A mono-window algorithm for retrieving land surface temperature from Landsat TM data and its application to the Israel-Egypt border region. *International Journal of Remote Sensing*, **22**, 3719–3746.

Richardson DM (1998) Forestry trees as invasive aliens. *Conservation Biology*, **12**, 18–26.

Ruimy A, Saugier B, Dedieu G (1994) Methodology for the estimation of terrestrial net primary production from remotely sensed data. *Journal of Geophysical Research*, **99**, 5263–5283.

Ryan MG, Binkley D, Fownes J (1997) Age related decline in forest productivity: patterns and process. *Advances in Ecological Research*, **27**, 213–262.

SAGPyA (1999) *Argentina, oportunidades de inversión en bosques cultivados*.

SAGPyA (2002) Primer inventario nacional de plantaciones forestales en macizo. *SAGPyA Forestal*, **20**.

Sahin V, Hall MJ (1996) The effects of afforestation and deforestation on water yields. *Journal of Hydrology*, **178**, 293–309.

Sanchez JM, Caselles V (2004) Determining actual evapotranspiration in a boreal forest. *Recent Research Developments in Geophysics*, **6**, 59–80.

Sanchez JM, Caselles V, Niclós R *et al*. (2003) Cálculo de la evapotranspiración en un bosque boreal. *Revista de Teledetección*, **20**, 53–57.

Sapanov MK (2000) Water uptake by trees on different soils in the Northern Caspian region. *Eurasian Soil Science*, **33**, 1157–1165.

Saurer M, Siegwolf RTW, Schweingruber FH (2004) Carbon isotope discrimination indicates improving water-use efficiency of trees in northern Eurasia over the last 100 years. *Global Change Biology*, **10**, 2109–2120.

Schenk HJ, Jackson RB (2002) The global biogeography of roots. *Ecologial Monographs*, **72**, 311–328.

Schott JR, Volchok WJ (1985) Thematic Mapper thermal infrared calibration. *Photogrammetric Engineering and Remote Sensing*, **51**, 1351–1357.

Schulze ED, Schulze W *et al*. (1995) Aboveground biomass and nitrogen nutrition in a chronosequence of prisitine Dahurian Larix stands in eastern Siberia. *Canadian Journal of Forest Research*, **25**, 943–960.

Scott RL, James Shuttleworth W, Goodrich DC *et al*. (2000) The water use of two dominant vegetation communities in a semiarid riparian ecosystem. *Agricultural and Forest Meteorology*, **105**, 241–256.

Scott DF, Lesch W (1997) Streamflow responses to afforestation with *Eucalyptus grandis* and *Pinus patula* and to felling in the Mokobulaan experimental catchments, South Africa. *Journal of Hydrology*, **199**, 360–377.

Seguin B, Baelz S, Monget JM *et al*. (1982) Utilisation de la thermographie IR pour l'estimation de l'évaporation régionale. I. Mise au point méthodologique sur la site de la Crau. *Agronomie*, **2**, 7–16.

Seguin B, Itier B (1983) Using midday surface temperature to estimate daily evaporation from satellite thermal IR data. *International Journal of Remote Sensing*, **4**, 371–383.

Sellers PJ (1985) Canopy reflectance, photosynthesis and transpiration. *International Journal of Remote Sensing*, **6**, 1335–1372.

Sepliarsky F, Dalla Tea F (1993) *Crecimiento de Eucalyptus grandis en relación con factores edáficos*. Congreso Forestal Argentino y Latinoamericano, Paraná, Argentina.

Shukla J, Nobre CA, Sellers P (1990) Amazonia deforestation and climate change. *Science*, **247**, 1322–1325.

Shuttleworth WJ (1993) Evaporation. In: *Handbook of Hydrology* (ed, Maidment DR), McGraw-Hill, New York.

Van de Griend AA, Owe M (1993) On the relationship between thermal emissivity and the normalized difference vegetation index for natural surfaces. *International Journal of Remote Sensing*, **14**, 1119–1131.

Vertessy RA, Watson FGR, O'Sullivan SK (2001) Factors determining relations between stand age and catchment water balance in mountain ash forests. *Forest Ecology and Management*, **143**, 13–26.

Vidal A, Kerr Y, Lagouarde JP *et al*. (1987) Teledetection et bilan hydrique: utilisation combinee d'un modele agrometeorologique et des donnees de l'IR thermique du satellite NOAA-AVHRR. *Agricultural and Forest Meteorology*, **39**, 155–175.

Vitousek PM (1977) The regulation of element concentrations in mountain streams in the northeastern US. *Ecologial Monographs*, **47**, 65–87.

Wright JA, DiNicola A, Gaitan E (2000) Latin American forest plantations – opportunities for carbon sequestration, economic development and financial returns. *Journal of Forestry*, **98**, 20–23.

Zhang L, Dawes WR, Walker GR (2001) Response of mean annual evapotranspiration to vegetation changes at catchment scale. *Water Resources Research*, **37**, 701–708.

## Appendix A

### *Net radiation estimates*

Net radiation (Rn), which can be separated in net short wave radiation (Sn) and long-wave radiation (Ln), was computed using geometrical calculations of solar radiation and satellite estimates of land surface albedo. Total incoming short-wave radiation (St) was calculated as (Shuttleworth 1993)

$$\mathrm{St} = \left(a + b\frac{m}{\mathrm{M}}\right)\mathrm{So}, \tag{A1}$$

where $m$ is the bright sunshine hours per day (h), $M$ is the total day length (h), and $a$ and $b$ are the constants that assume values of 0.25 and 0.50 for average climates, respectively. Extraterrestrial solar radiation (So) (mm day$^{-1}$) was calculated as

$$\mathrm{So} = 15.392\, d_\mathrm{r}(\omega_s \sin\phi \sin\delta + \cos\phi \sin\omega_\mathrm{s}), \tag{A2}$$

where $d_\mathrm{r}$ is the relative distance between the earth and the sun, $\omega_\mathrm{s}$ the sunset hour angle, $\phi$ the site latitude, and $\delta$ the solar declination. Net shortwave radiation was calculated as

$$\mathrm{Sn} = \mathrm{St}(1-\alpha), \tag{A3}$$

where surface albedo ($\alpha$) was computed from bands 1, 3, 4, 5, and 7 of Landsat images following the methods outlined by Liang (2000).

Net long-wave radiation was estimated empirically according to Granger & Gray (1990). For a natural surface, the fluctuations in surface and atmospheric temperatures and, to a large extent, the variations in atmospheric humidity are driven by the energy supplied to the surface; so, for clear sky conditions and daily values, Ln can be estimated from incoming short-wave radiation as

$$\mathrm{Ln} = -4.25 - 0.24\,\mathrm{St}. \tag{A4}$$

Net all-wave radiation (Rn) is the sum of its short-wave and long-wave components (Eqns (A3) and (A4)).

### *Surface and air temperature estimates*

A mono-window algorithm developed by Qin *et al*. (2001) was used to retrieve the surface temperature ($T_\mathrm{s}$) from Landsat images. The algorithm has the following form:

$$T_\mathrm{s} = \{h(1-C-D) + [k(1-C-D)+C+D]T_\mathrm{b} - DT_\mathrm{a}\}/C, \tag{A5}$$

where $T_\mathrm{a}$ is the effective atmospheric mean temperature, which can be determined from the air temperature ($\sim$2 m height) by the method in Qin *et al*. (2001), $T_\mathrm{b}$ is the effective at-satellite brightness temperature, $h$ and $k$ are the constants needed to linearize Planck's radiance equation, given as $h = -67.35535$ and $k = 0.45861$, and the parameters $C$ and $D$ are defined as

$$C = \varepsilon\tau, \tag{A6}$$

$$D = (1-\tau)[1 + (1-\varepsilon)\tau], \tag{A7}$$

where $\varepsilon$ is the ground emissivity, which was computed from NDVI according to Van de Griend & Owe (1993), and $\tau$ is atmospheric transmittance, estimated from water vapor content following Qin *et al*. (2001). Satellite brightness temperature for each pixel was calculated using the following relationship, similar to the Planck equation with two free parameters (Schott & Volchok 1985):

$$T_\mathrm{b}\left[\frac{K_2}{\mathrm{Ln}\left(\frac{K_1}{L}+1\right)}\right], \tag{A8}$$

where $L$ is the blackbody radiance for temperature $T_\mathrm{b}$, integrated over the ETM + band-6, $K_1 = 666.09$ W m$^{-2}$ sr$^{-1}$ mm$^{-1}$, and $K_2 = 1282.71$ K (Irish, 2000).

In their original approach Carlson *et al*. (1995) used temperature differences ($T_\mathrm{s}-T_\mathrm{a}$) measured close to noon (13:00 hours). Because Landsat images correspond to an earlier time of the day (10:30 hours), we evaluated the possibility of using $(T_\mathrm{s}-T_\mathrm{a})_{10:30\ \mathrm{hours}}$ as a surrogate of $(T_\mathrm{s}-T_\mathrm{a})_{13:00\ \mathrm{hours}}$ by comparing the values over different covers (grasses, trees, bare soils) on clear sky conditions based on field measurements performed with a handheld infrared thermometer (Raytek ST20, Raytek Co., Santa Cruz, CA, USA) and a pocket thermowind meter (Kestrel 2000, Nielsen-Kellerman Co., Boothwyn, PA, USA). Measurements at both times were strongly correlated ($r^2 = 0.95$, $n = 72$) with the slope and origin of the relationship being not statistically different from one ($P = 0.92$) and zero ($P = 0.95$), respectively. Inoue & Moran (1997) arrived at the same results comparing measurements performed on crops between 10:30 and 14:00 hours.

*Exchange coefficient and correction for non-neutral static stability*

The exchange coefficient ($B$) in the evapotranspiration equation represents an average bulk conductance for daily-integrated sensible heat flux, and the $n$ coefficient is a correction for non-neutral static stability and is generally assigned a value close to one (Seguin & Itier 1983). The value of $B$ depends on the roughness and wind velocity; so assigning a single value for different vegetation types is unacceptable. Carlson & Buffum (1989) indicated that $B$ is much more sensitive to the amount of vegetation, which can be accurately estimated from a scaled vegetation index NDVI*, where

$$\mathrm{NDVI}^* = \left(\frac{\mathrm{NDVI} - \mathrm{NDVI}_{\min}}{\mathrm{NDVI}_{\max} - \mathrm{NDVI}_{\min}}\right), \tag{A9}$$

$$\mathrm{NDVI} = \frac{\rho_{\mathrm{NIR}} - \rho_{\mathrm{RED}}}{\rho_{\mathrm{NIR}} + \rho_{\mathrm{RED}}} \tag{A10}$$

$\rho_{\mathrm{NIR}}$ and $\rho_{\mathrm{RED}}$ being the reflectance in the near-infrared and in the red, and $\mathrm{NDVI}_{\min}$ is the NDVI for bare soil, and $\mathrm{NDVI}_{\max}$ is the NDVI with dense vegetation. Later, Carlson *et al*. (1995), working with a soil–vegetation–atmosphere transfer (SVAT) model, proposed the following equations for the coefficients $B$ and $n$:

$$n = 1.067 - 0.372\,(\mathrm{NDVI}^*), \tag{A11}$$

$$B = 0.0109 + 0.051\,(\mathrm{NDVI}^*). \tag{A12}$$

Using these relationships we obtained a mean $B$ value of $0.56\,\mathrm{mm\,day^{-1}\,K^{-1}}$ for tree plantations and $0.27\,\mathrm{mm\,day^{-1}\,K^{-1}}$ for grasslands, which are in agreement with previous work (Seguin & Itier 1983; Sanchez *et al*., 2003).